The phi complex as a neuromarker of human social coordination

Emmanuelle Tognoli*, Julien Lagarde*†, Gonzalo C. DeGuzman*, and J. A. Scott Kelso*‡

*Human Brain and Behavior Laboratory, Center for Complex Systems and Brain Sciences, Florida Atlantic University, Boca Raton, FL 33431; and †Efficience Déficience Motrices, Université Montpellier-1, 34090 Montpellier, France

Edited by Michael I. Posner, University of Oregon, Eugene, OR, and approved March 26, 2007 (received for review December 22, 2006)

Many social interactions rely upon mutual information exchange: one member of a pair changes in response to the other while at the same time producing actions that alter the behavior of the other. However, little is known about how such social processes are integrated in the brain. Here, we used a specially designed dual-electroencephalogram system and the conceptual framework of coordination dynamics to identify neural signatures of effective, real-time coordination between people and its breakdown or absence. High-resolution spectral analysis of electrical brain activity before and during visually mediated social coordination revealed a marked depression in occipital alpha and rolandic mu rhythms during social interaction that was independent of whether behavior was coordinated or not. In contrast, a pair of oscillatory components (phi_1 and phi_2) located above right centro-parietal cortex distinguished effective from ineffective coordination: increase of phi_1 favored independent behavior and increase of phi_2 favored coordinated behavior. The topography of the phi complex is consistent with neuroanatomical sources within the human mirror neuron system. A plausible mechanism is that the phi complex reflects the influence of the other on a person's ongoing behavior, with phi_1 expressing the inhibition of the human mirror neuron system and phi_2 its enhancement.

brain oscillations | electroencephalography | mirror neuron system | phi rhythm | coordination dynamics

Two anatomically overlapping yet functionally distinct systems in the brain have been identified when we interact with others. The first, historically called the motor preparation system, consists of cortical circuitry that includes the premotor cortex, the supplementary motor area, and parts of the inferior parietal cortex (1). This system is deemed responsible for implementing the intention to realize one's own actions (2, 3). The second, the mirror-neuron system (4, 5), allows for the actions of others to be perceived (6), embodied (7), understood (8, 9), and appropriated (10) by our own motor system. Its main components are the inferior parietal sulcus, the premotor cortex (5, 11, 12), and the superior temporal sulcus (STS) (although the motor properties of STS neurons coactivated during observation and execution are presently the subject of some debate; see ref. 6). In evolutionary terms, the mirror-neuron system may facilitate important functions of skill learning, language acquisition, everyday joint action, and interpersonal coordination (13). A common viewpoint (5, 14) is that the mirror-neuron system is inactive most of the time but is activated upon request. Research on pathological imitation (15) suggests a further possibility, namely, that the mirror-neuron system is constantly available for use but is actively suppressed by inhibition (16).

Neurophysiological studies of the influence of one person's actions on another have so far assessed the behavioral acts of pairs of individuals one at a time, i.e., one acts while the other observes; or one acts but only later does the other imitate (17–24). In many everyday social interactions, however, one member of a pair changes in response to the other while at the same time producing actions that alter the behavior of the other (25, 26). What neural mechanisms underlie such real-time coordination between people, and how might they be identified? Here, we used a specially designed dual-electroencephalogram (EEG) system in an experimental paradigm (ref. 27; see also ref. 28) that allows both individual and social (interpersonal) tendencies to be quantified continuously in time. Our approach stems from coordination dynamics, an empirically based theoretical framework that aims to understand how patterns of coordination form, adapt, persist and change at multiple levels of brain and behavioral function (e.g., refs. 29–39). Such self-organized pattern formation in the brain is a subject of much active investigation in the neurosciences and expresses itself in various forms, including brain oscillations (e.g., refs. 40–42), transient phase synchrony among neural populations (30, 38, 43–47), multistability, abrupt phase transitions ("switches") in behaviorally induced cortical activity patterns (48–53), and so forth. A positive contribution of coordination dynamics to understanding the brain-behavior relation is that it has been able (*i*) to identify key coordination or collective variables for complex patterns of behavior; and (*ii*) to derive patterns of collective behavior from the coupling among interacting components at both behavioral and brain levels (see refs. 33 and 54 for reviews).

As a framework specifically geared to handle informationally coupled self-organizing systems, coordination dynamics is well suited for studying how social coordination emerges from individual behavior in real time (see, e.g., refs. 27, 55, and 56). In the present study, we employed a rhythmic task in which pairs of subjects move their fingers at their own preferred frequency and amplitude with and without vision of the other's movements. Previous behavioral studies have shown that unintended spontaneous coupling may occur (manifest in transitions from independent to phase-locking behavior) when subjects see each other's hand movements (27, 55). Here, we explored the neural underpinnings of such social coordination: along with relative phase measures to precisely quantify the informational exchange between people, we employed high-resolution spectral measures of their brain activity. As a consequence thereof, we identified three distinct EEG rhythms, one of which (located over right centro-parietal cortex) "neuromarks" the presence or absence of social coordination.

Results

Eight pairs of participants executed self-paced rhythmic finger movements with and without vision of each other's actions. The movements and neuroelectric activity of both members of the pair were continuously monitored and recorded at a time scale

Author contributions: E.T., J.L., G.C.D., and J.A.S.K. designed research; E.T. and J.L. performed research; E.T., J.L., G.C.D., and J.A.S.K. analyzed data; and E.T., J.L., G.C.D., and J.A.S.K. wrote the paper.

The authors declare no conflict of interest.

This article is a PNAS Direct Submission.

Freely available online through the PNAS open access option.

Abbreviations: EEG, electroencephalogram; LC, liquid crystal; CV, circular variance.

‡To whom correspondence should be addressed. E-mail: kelso@ccs.fau.edu.

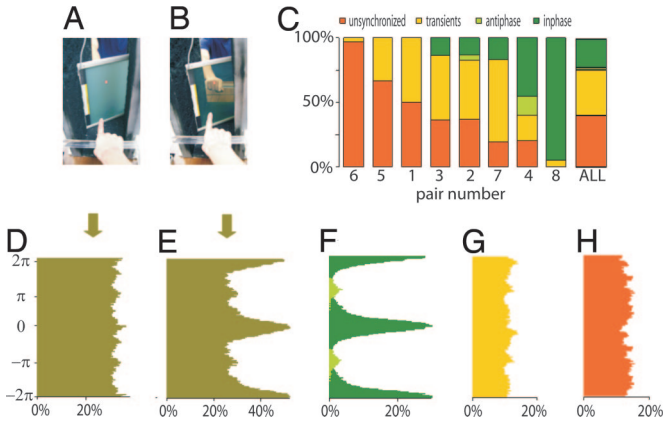

Fig. 1. The experimental setting and behavioral findings. Visual contact between subjects is manipulated by turning on (*A*) and off (*B*) a liquid crystal screen. (*C*) Distribution of trials for all eight pairs of subjects, arranged in increasing degree of coordination. An index (γ_{cv}) based on circular variance was used to assess the strength of coordination. Orange bars represent unsynchronized behavior ($\gamma_{cv} < 0.03$); green bars are from synchronized trials ($\gamma_{cv} > 0.73$). Dark and light green signify in-phase and anti-phase synchronization, respectively. Yellow bars represent transient behavior. The overall relative phase distributions for all trials corresponding to the vision-off and vision-on segments are shown in *D* and *E*, respectively. By using similar color coding as in *C*, further decompositions into synchronized (*F*), transient (*G*), and unsynchronized (*H*) trials are displayed.

that enabled us to observe evolving patterns of behavioral and brain activity. Periods of social interaction ("vision-on," 20-s duration) were framed by two 20-s control periods ("vision-off") during which participants' sight of each other was blocked. Vision was controlled by using a liquid crystal (LC) screen panel, interposed between participants, the opacity of which could be electronically switched on and off (see Fig. 1 *A* and *B*).

Vision of the other created the opportunity for a transition from independent to coordinated behavior: accordingly, the distribution of the relative phase of finger movements during vision-on (Fig. 1*E*) showed some concentration at 0 (modulo 2π), and pi (modulo 2π), expressing tendencies for synchronizing in-phase (fingers of both participants reaching their peak flexion at the same time) and anti-phase (finger of one participant reaching peak extension at the same time that the other reaches peak flexion). This relative phase concentration was absent during vision-off (Fig. 1*D*).

Trials were classified into three categories: fully synchronized, transiently synchronized, and unsynchronized, quantitatively verified by using an index of synchronization γ_{cv} (see *Materials and Methods*). Social coordination was defined when the relative phase of the finger movements entered a stable phase-locked state shortly after visual contact (<2 s) and persisted over the entire period of visual contact. Transient synchronization was defined when brief episodes of phase locking were observed during the period of visual contact but were not maintained throughout the period. Unsynchronized behavior was defined by the persistent absence of phase locking across the entire period of visual contact. Fig. 1*C* shows the distribution of the trials based on the three categories of behavior: synchronized, transient, and unsynchronized. Trials of fully synchronized behavior accounted for 25% of all of the trials (Fig. 1*F*). Transient phase locking was observed in 37% of the trials (Fig. 1*G*). Both synchronized and transient trials showed tendencies toward in-phase and anti-phase patterns, reminiscent of many studies of rhythmic sensorimotor coordination in individual subjects (e.g., refs. 32 and 57–65). Unsynchronized trials comprised 38% of the total and were characterized by a complete absence of phase-locking tendencies (Fig. 1*H*). No phase attraction means that subjects essentially retained their own rhythm and were unaffected by the visual input of the other's movements.

Coordination behavior was verified visually and numerically by using a synchronization index based on the relative phase circular variance (66). This index is a unit-normalized number, with 0 describing the absence of synchronization and 1 describing full synchronization. Synchronized trials had an index >0.73 whereas unsynchronized ones had an index of <0.03. Transient behavior was in between, with synchronization index values ranging from 0.03 to 0.75 (Fig. 1*G*). Notice that the index is a measure of the net strength of the interaction arising from the individual intrinsic dynamics (reflected in the frequency and amplitude of movement chosen before visual contact) and the mutual coupling.

Neural correlates of synchronized and unsynchronized behaviors were sought by using high-resolution spectral analysis (0.06-Hz steps). The rationale was that emergent coordinative behaviors, whether synchronized or unsynchronized, would be sustained by at least one of the subjects in the pair. Accordingly, we expected to identify neural signatures of social coordination by observing corresponding EEG spectral changes. By using the visualization method described in *Materials and Methods*, three categories of spectra with distinct topography were identified in the 7.5- to 13-Hz range (Fig. 2 *A* and *B*): alpha (mean frequency of 10.61 Hz), mu (mean frequency of 9.63 Hz), and a lateralized centro-parietal component that we call phi (spanning the range 9.2–11.5 Hz; Fig. 2*B*). In 11 subjects, separable peaks were observed for at least one of the three brain rhythms (Fig. 2*B*).

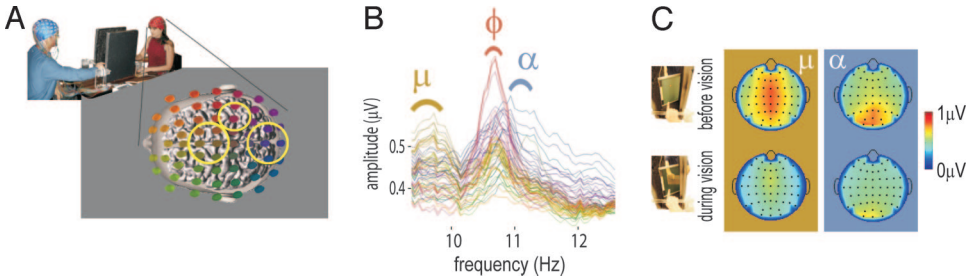

Fig. 2. Identification of spectral components in the brain activity of participants. (*A*) The dual-EEG of pairs was recorded with two caps each containing 60 channels. The head schematic of the subject on the right shows the 60 electrodes color-coded to reflect their spatial location. A similar identification was conducted on the second participant's EEG (data not shown). Circled areas indicate regions of peak rhythmic activity: mu (electrodes colored brown situated above Rolandic fissure); phi (burgundy above right centro-parietal area); and alpha (blue above the occipital pole). (*B*) Spectral plots used to identify mu, phi, and alpha components during visual contact. Because behavior in this example was completely unsynchronized, spectra show only phi_1, mu, and alpha, but no noticeable phi_2. (*C*) Topographical distributions of the mu and alpha rhythms before (*Upper*) and during (*Lower*) vision. The power of rolandic mu and posterior alpha was significantly depressed during visual contact, independently of the coordination achieved by each pair.

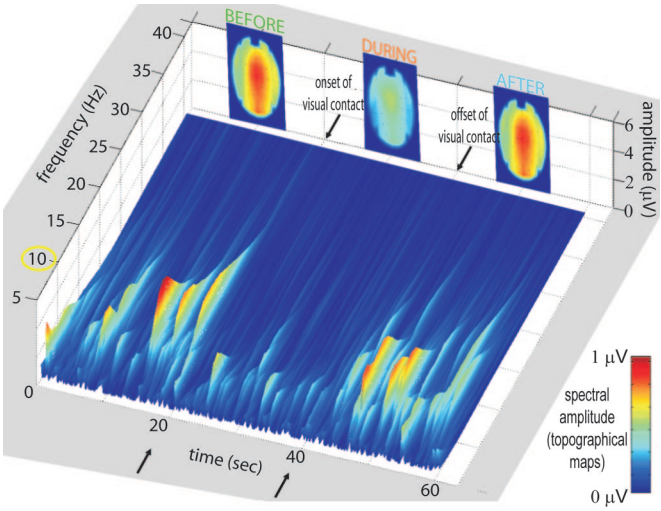

Fig. 3. Time-frequency spectrum exhibiting vanishing bursts in the 10-Hz range during visual contact (from $t = 20$ to $t = 40$ s). The topographical maps at the top of the figure show the total energy in the range 9–11 Hz and capture both mu and alpha processes before and after vision and their desynchronization during vision. In this particular subject, no phi complex was detected. However, a wide spectral maximum at 11–14 Hz over occipital areas and an ample but narrow spectral maximum centered at 9.2 Hz over rolandic areas were observed.

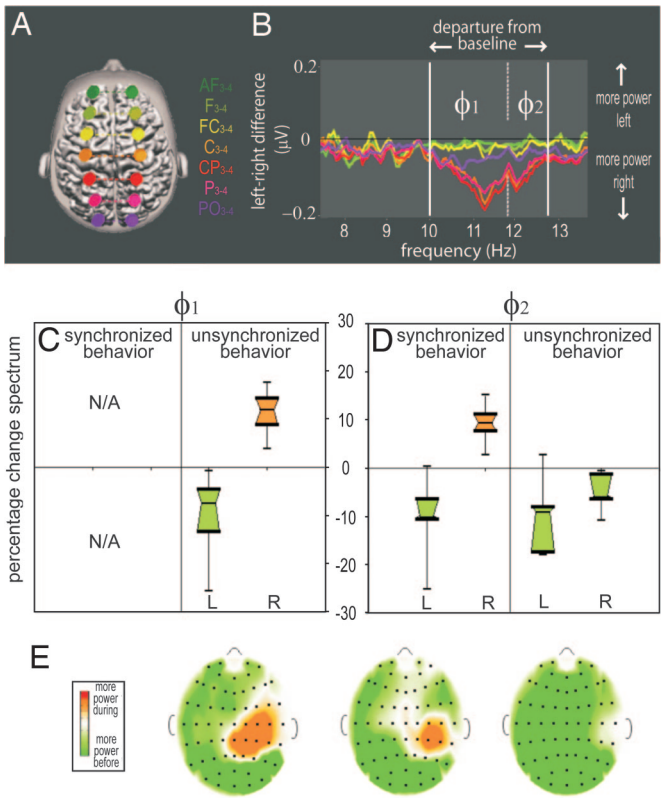

Fig. 4. Phi_1 and Phi_2 rhythms distinguish synchronized and unsynchronized (intrinsic) behavior. (*A*) Electrodes used to identify the phi complex are located 6 cm from the midline. (*B*) Plots of power differences between matching left and right electrodes of *A*. Because of their symmetry, most spectral components cancel out and only the asymmetrical components are retained. (*C*) Box-and-whiskers plot of power changes in Phi_1 showing selective increase in the right hemisphere and a corresponding decrease in the left hemisphere during unsynchronized behavior. (*D*) For Phi_2, power selectively increases in the right hemisphere only during synchronized behavior. Note the absence of overlap between the active phi distributions in the right hemisphere and their controls in the left hemisphere. (*E*) Representative examples of corresponding maps of power change showing that the topography of Phi_1 (unsynchronized behavior) and Phi_2 (synchronized behaviors) are similar. L, left hemisphere; R, right hemisphere.

In particular, phi was observed in all 11 subjects, 10 with right and 1 with left lateralization. Phi appeared at a single brain location but typically involved a double peak in the spectral domain (Fig. 4 *A* and *B*).

Although alpha and mu showed a significant decrease (alpha, −30.4%; mu, −20.1%) during visual contact as compared with before visual contact (alpha at POz, $Z = -2.67$, $P < 0.008$; mu at FCz, $Z = -2.1$, $P < 0.036$; Fig. 2*C*), neither rhythm was specifically modulated by the strength of the coordination *per se*. Specifically, these rhythms displayed intermittent bursting before and after visual contact and were suppressed during vision (Fig. 3).

In contrast, the phi complex was highly sensitive to the characteristics of social coordination achieved during visual contact. Increase of the first component was specific to unsynchronized behavior; increase of the second component was specific to synchronized behavior (Fig. 4 *C* and *D*).

In a number of cases during which the spectral amplitude of mu and/or alpha was small, we were able to identify changes in the dynamics of the phi complex associated with changes in behavioral coordination (Fig. 5). Such cases support the causality between the phi complex and social coordination.

Discussion

Consistent with previous studies of behavior alone (27, 55), spontaneous coordination in the form of synchronized behavior was observed between participants during visual contact even though no instruction to coordinate was given. Vision of the other's movements created an opportunity to couple, often inducing a transition from independent to coordinated behavior. Interestingly, the discrete set of stable-phase relations observed (in-phase and anti-phase) indicated that basic symmetries are at work even between two people (28, 60, 67). For social coordination qua phase-locking to occur, at least one of the participants has to be influenced by vision of what the other is doing. In neural terms, the mirror-neuron system must effectively influence the motor cortex of at least one participant (68, 69). In contrast, when no phase-locking tendency is observed individual behaviors ("intrinsic dynamics") predominate (33), presumably by enhancing activity in the premotor system or by inhibiting the mirror-neuron system. Our results suggest that phi_1 reflects the inhibition of the mirror-neuron and/or the enhancement of intrinsic premotor activity, whereas phi_2 reflects the enhancement of the mirror-neuron system and/or the inhibition of intrinsic premotor activity. Potential sources for the centroparietally located phi complex include areas reported to belong to the human mirror-neuron system, in particular parietal areas and the superior temporal sulcus (4, 5, 9, 10, 17, 70–81). The presence of a complex formed by two distinct peaks is an unusual spectral feature of human EEG. It could express the activation of largely overlapping networks (e.g., motor preparation and mirror neuron systems) so that the observed proximity in both the spectra and topography is attributed to the common parts; or it could indicate a frequency shift of a single oscillation because of coupling with remote processes.

The present results show that, although mu and alpha are consistently depressed by the perception of the other's movement, they are insensitive to social coordination or its absence. Both mu and alpha rhythms have been described as functional correlates of resting brain states and arise from the hyperpolarization of thalamo-cortical relay cells (82). Alpha desynchroni-

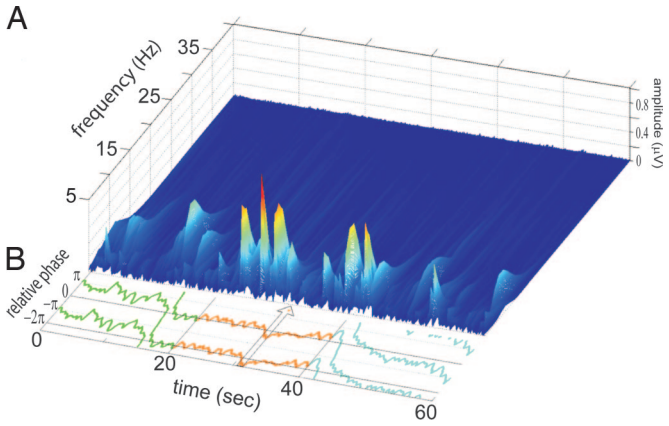

Fig. 5. Relation between Phi_2 and social coordination. (*A*) Time-frequency spectrum for electrode CP4 from a single trial. Phi_2 is low before and after vision but increases during vision. (*B*) Corresponding relative phase between finger movements. Synchronized in-phase behavior is observed most of the time during visual contact. The momentary loss of coordination around $t = 31$ s (highlighted by the arrow) is associated with the disappearance of Phi_2, seen by the gap from time $t = 30$ to $t = 35$ s in the time-frequency spectra.

zation is observed during attentive vision (83, 84) whereas mu desynchronization is typically observed in a broad range of sensorimotor activities that includes execution, observation, and somatosensory stimulation (18, 20, 85–91).

Recently, the mu rhythm has been proposed as an electrophysiological correlate of mirror-neuron activity in normal (20, 87, 92) and pathological populations (88). The anatomical and functional distinction between mu and the phi complex revealed here sheds light on this hypothesis: high-resolution spectral analysis indicates that rolandic mu does not show any departure from the midline and does not engage specifically during social coordination (Fig. 2*C*). To the contrary, our data suggest that the mirror-neuron system effects appropriate behavioral changes by recruiting an oscillatory complex that is spatially and spectrally distinct from rolandic mu.

In short, our results suggest that mu and phi both constitute neural correlates of the human mirror-neuron system but play distinctly different roles. Whereas mu contributes to somatosensory awareness when the acting partner is perceived (85, 93), the phi complex plays the role of a gating mechanism, selectively parsing social from individual, so-called "intrinsic" behavior. Phi thus appears as a robust neuromarker or signature of social coordination, at least for the very basic forms of social interaction that emerge when people couple spontaneously with each other. Whether phi is unique and specific to social behavior or is a multifunctional mechanism shared with other forms of perceptuo-motor coupling, even with nonhuman agents (94) is, of course, open to further test. Likewise, the present approach clears the way for future investigations of a broad range of factors that may influence the tendency to coordinate, ranging from basic kinematic differences between movements of participants to high-level social factors such as trust (95). The functional dissociation among brain rhythms observed here may be important not only for the field of normal social cognition (96) but also for understanding pathologies where antagonistic results are currently translated into theories (e.g., between mu and mirror-neuron system deficits) and are on the verge of guiding therapeutic targeting.

Materials and Methods

Subjects. Sixteen subjects (10 males and 6 females; aged between 22 and 41 years, mean 29 years) participated in the experiment. They constituted eight pairs: four gender-mixed; three male–male; and one female–female. All were right-handed on the basis of self-report. They had normal or corrected-to-normal vision and reported no history of neurological disease. The protocol was approved by the Florida Atlantic University ethical board and was in agreement with the Declaration of Helsinki. Informed consent was obtained from all subjects.

Task. Pairs of subjects sat in front of each other while executing self-paced rhythmic finger movements during one-minute trials. An LC screen (Alumiglass, FL) with switchable opacity (switching time <1.2 ms) was placed between subjects to control vision of the other's motion. A trial consisted of three successive phases each lasting 20 s: before-vision, with the LC screen opaque (Fig. 1*A*), during-vision, with the LC screen transparent (Fig. 1*B*), and after-vision, with the screen back to opaque again (Fig. 1*A*). The LC screen was electronically controlled by means of a computer running the Experimental Run Time System (ERTS; Berisoft, Germany) software for optimal timing accuracy. Subjects were instructed to adopt the movement frequency that they felt most comfortable with and to maintain the fixation over a central spot on the LC screen. When the screen was transparent, the spot was in the same azimuth as the hand of the other participant. EEG artifacts induced by posture or finger movements were minimized before each trial. A trial started with two auditory cues presented in succession, one to each subject, signaling the respective recipients to commence rhythmically moving their index fingers at their preferred frequency and amplitude. The auditory warning cues were delivered through separate ear pieces 2 s (±0.5 s, random distribution) and 1 s (±0.5 s, random distribution) before the onset of the first 20-s period. The variable delay set a random initial relative phase between subjects and prevented common phase priming in the movements. The experiment consisted of 36 trials, with at least a 30-s rest between trials.

EEG Recording. The experiment was conducted in a sound-proof Faraday chamber. Dual-EEG was recorded by using two 60-channel EEG caps with Ag-AgCl electrodes (Falk Minow Services, Germany) arranged according to the 10% system (97) including midline and rows 1–8. The signals were fed to a single amplifier (Synamp2; Neuroscan, TX) equipped with two distinct referential montages. This specially designed dual-EEG system ensured no delays between the EEGs acquired from each subject and allowed precise analyses of cortical activity. EEG signals were measured with the respective grounds located at FPz sites and the references at the corresponding linked mastoids. Impedances were maintained below 10 kΩ (98). The signals were analog filtered (Butterworth, bandpass from 0.05 Hz (−12 dB per octave) to 200 Hz (−24 dB per octave), amplified (gain of 2,010) and digitized at 1,000 Hz with a 24-bit ADC in the range ±950 μV (vertical resolution of 0.11 nV).

Movement Recording. For finger movement data, angular change at the metacarpophalangeal joint was recorded by means of light single-axis goniometers (Biometrics, Ltd., U.K.) affixed to the right index finger of each subject. These signals were acquired through the high level port of the Neuroscan Synamp 2 bioamplifier, with an online bandpass filtering at a common EEG analog filter setting (0.05–200 Hz).

Behavioral Analysis and Statistics. Movement data were preprocessed by using a digital low-pass filter (Butterworth; 10 Hz, 24 dB) applied in a two-pass recursive manner to achieve zero-phase shift. The relative phase between the fingers was computed by using the continuous Hilbert transforms of the mean-centered time series. On the basis of the movement profiles during the visual contact period, the trials were initially classified by three experts into three categories: synchronized, transiently

synchronized, and unsynchronized trials. The classifications were further refined and numerically checked by using the synchronization index γ_{cv} based on the circular variance (CV) (66) of the relative phase. Note that this measure is sensitive to variations of the phase of the time series and not to the amplitudes. For N data points, the index is defined as

$$\gamma_{cv} \equiv \frac{1}{N}\left|\sum_{k=1}^{N} e^{i(\theta_k^{(1)}-\theta_k^{(2)})}\right| = 1 - CV, \qquad [1]$$

where $\theta_k^{(1)}$ and $\theta_k^{(2)}$ are the Hilbert phases for the subject pair at time k and CV is the circular variance of the differences $\theta_k^{(1)} - \theta_k^{(2)}$. If the phases follow each other closely at all times (highly synchronized), $\theta_k^{(1)} - \theta_k^{(2)} \approx \delta$ for some constant δ, and γ_{CV} is close to one. For fully unsynchronized and uncoupled systems, γ_{CV} tends to 0. A lower bound and an upper bound for γ_{CV} were used to discriminate between synchronized and unsynchronized trials, respectively. Note that the index is a measure of the net strength of the interaction arising from the individual intrinsic dynamics (reflected in the frequency and amplitude of movement chosen before visual contact) and the mutual coupling.

EEG Spectral Analysis. Classical studies of EEG oscillations are often performed (*i*) at low spectral resolutions by using fast Fourier transform (FFT) on samples of a few hundreds of milliseconds; (*ii*) within large frequency bands (typically 2–3 Hz in the alpha range); and (*iii*) without access to the inter-individual variability in the frequency of the rhythms. Our paradigm allowed us to investigate rhythms over a period of 16.5 s from each 20-s segment of a trial (a 3-s transient at the onset and a 0.5-s transient at the end were removed as the brain activity was expected to be nonstationary near these boundaries), resulting in a spectral resolution of 0.06 Hz. Single trials were tapered with a Tukey window (10%), and discrete Fourier transforms (DFT) were used to estimate amplitude spectra. For display purposes, the spectra were smoothed with a 5-point Bartlett filter. Oscillatory processes in the brain were isolated on a subject-by-subject basis by using the following procedures.

Power asymmetry. The difference in the spectral amplitudes between the interhemispheric pairs of electrodes in rows 3 and 4 of the 10%-montage (97) (e.g., difference C3–C4 over the central sulcus) was computed. Symmetrical rhythms canceled out, and the phi complex was isolated because of its asymmetry. Active phi components (components increasing their amplitude during visual contact in synchronized or unsynchronized behaviors) were identified, and their changes in power, event-related desynchronization (ERD) and event-related synchronization (ERS) (99), were examined further.

Occipital and central rhythms. Waking EEG is characterized by a $1/f^{\alpha}$ spectrum (100), over which a few peaks appear. Those peaks express the underlying presence of a specific functional network operating at defined frequencies. We defined spectral peaks as maxima in the spectrum in excess of the $1/f^{\alpha}$ trend. The presence of the occipital/rolandic maxima in the range 7.5–13Hz was determined by visual inspection, and their boundaries/amplitude were extracted.

EEG Time-Frequency Analysis. The spectral density over the time course of individual trials was also investigated. The spectral amplitude in the time-frequency plane was computed by using a continuous wavelet transform (CWT). For the mother function of the transform, we chose the complex Morlet wavelet $\psi(x)$

$$\psi(x) = \sqrt{\pi f_b}\, e^{2i\pi f_c x} e^{-\frac{x^2}{f_b}}, \qquad [2]$$

where f_c is the center frequency and f_b is frequency bandwidth. The Morlet wavelet is a complex sinusoidal function tapered with a Gaussian window and is optimal for sinusoidal-shaped oscillations such as alpha. It can also detect periodic signals of different morphologies such as mu but with lower spectral definition and leakage of parts of the power into additional/other components.

EEG Artifacts. Eye blinks are large-amplitude EEG components whose waveshapes resemble positively skewed Gaussians, sometimes associated with final undershoots. The typical duration of an eye blink is 200–400 ms, and its spectral signature spans the delta and theta range (101, 102), with most of the energy residing below 5 Hz. Muscle artifacts arise from the fluttering of the electrodes in the vicinity of active neck and face muscle groups and span the frequency range from the beta band up to ≈500 Hz (103, 104). The spectral characteristics of these two contaminants (eye blinks and muscle artifacts) have no overlap with the frequency bands investigated here. In agreement with Wallstrom's report (105) of induced second-order artifacts when correcting for primary contaminants (and especially in the alpha band), we did not employ correction techniques (e.g., regression, filtering, and decomposition) on the data.

We thank W. McLean for technical assistance and two anonymous reviewers for comments and suggestions. This work was supported by National Institute of Mental Health Grant MH42900 (to J.A.S.K.) and Office of Naval Research Grant N00014-05-1-0117 (to J.A.S.K. and Betty Tuller). J.L. was supported by Enactive Interfaces, a network of excellence (Information Society Technologies Contract 002114) of the Commission of the European Community.

1. Elsinger CL, Harrington DL, Rao SM (2006) *NeuroImage* 31:1177–1187.
2. Boussaoud D (2001) *NeuroImage* 14:S40–S45.
3. Lau HC, Rogers RD, Haggard P, Passingham RE (2004) *Science* 303:1208–1210.
4. Rizzolatti G, Fadiga L, Gallese V, Fogassi L (1996) *Cognit Brain Res* 3:131–141.
5. Rizzolatti G, Craighero L (2004) *Annu Rev Neurosci* 27:169–192.
6. Puce A, Perrett D (2003) *Philos Trans R Soc London A* 358:435–445.
7. Barsalou LW, Niedenthal PM, Barbey AK, Ruppert JA (2003) in *The Psychology of Learning and Motivation*, ed Ross BH (Academic, San Diego), pp 43–92.
8. Frith C, Frith U (2005) *Curr Biol* 15:R644–R645.
9. Fogassi L, Ferrari PF, Gesierich B, Rozzi S, Chersi F, Rizzolatti G (2005) *Science* 308:662–667.
10. Iacoboni M, Koski L, Brass M, Bekkering H, Woods RP, Dubeau MC, Mazziotta JC, Rizzolatti G (2001) *Proc Natl Acad Sci USA* 98:13995–13999.
11. Decety J, Grèzes J (1999) *Trends Cognit Sci* 3:172–178.
12. Giese MA, Poggio T (2003) *Nat Rev Neurosci* 4:179–192.
13. Stamenov M, Gallese V, eds (2002) *Mirror Neurons and the Evolution of Brain and Language*, Advances in Consciousness Research (John Benjamins, Philadelphia), Vol 42.
14. Gallese V, Keysers C, Rizzolatti G (2004) *Trends Cognit Sci* 8(9):396–403.
15. Lhermitte F, Pillon B, Serdaru M (1986) *Ann Neurol* 19:326–334.
16. Brass M, Derrfuss J, von Cramon DY (2005) *Neuropsychologia* 43:89–98.
17. Iacoboni M, Woods RP, Brass M, Bekkering H, Mazziotta JC, Rizzolatti G (1999) *Science* 286:2526–2528.
18. Cochin S, Barthelemy C, Roux S, Martineau J (1999) *Eur J Neurosci* 11:1839–1842.
19. Buccino G, Canessa N, Patteri I, Lagravinese G, Benuzzi F, Porro CA, Rizzolatti G (2004) *J Cognit Neurosci* 16:114–126.
20. Muthukumaraswamy SD, Johnson BW, McNair NA (2004) *Cognit Brain Res* 19:195–201.
21. Mühlau M, Hermsdörfer J, Goldenberg G, Wohlschläger AM, Castrop F, Stahl R, Röttinger M, Erhard P, Halinger B, Ceballos-Baumann AO, *et al.* (2005) *Neuropsychologia* 43:1086–1098.
22. Chaminade T, Meltzoff AN, Decety J (2005) *Neuropsychologia* 43:115–127.
23. Lepage JF, Théoret H (2006) *Eur J Neurosci* 23(9):2505–2510.
24. Calmels C, Holmes P, Jarry G, Hars M, Lopez E, Paillard A, Stam CJ (2006) *Hum Brain Mapp* 27(3):251–266.
25. Hamilton A, Wolpert DM, Frith U, Grafton ST (2006) *NeuroImage* 29:524–535.

26. Marsh KL, Richardson MJ, Baron RM, Schmidt RC (2006) *Ecol Psychol* 18:1–38.
27. Oullier O, de Guzman GC, Jantzen KJ, Lagarde JF, Kelso JAS, *Social Neurosci*, in press.
28. Schmidt RC, Carello C, Turvey MT (1990) *J Exp Psychol Hum Percept Perform* 16(2):227–247.
29. Beek PJ, Peper CE, Stegeman DF (1995) *Hum Movement Sci* 14:573–608.
30. Fingelkurts AA, Fingelkurts AA (2004) *Int J Neurosci* 114:843–862.
31. Jirsa VK, Kelso JAS (2004) *Coordination Dynamics: Issues and Trends* (Springer, New York).
32. Meyer-Lindenberg A, Ziemann U, Hajak G, Cohen L, Berman KF (2002) *Proc Natl Acad Sci USA* 99:10948–10953.
33. Kelso JAS (1995) *Dynamic Patterns: The Self-Organization of Brain and Behavior* (MIT Press, Cambridge MA).
34. Schöner G, Kelso JAS (1988) *Science* 239:1513–1519.
35. Singer W (2005) *MaxPlanckResearch* 3:S14–S18.
36. Tschacher W, Dauwalder JP (2003) *The Dynamical Systems Approach to Cognition: Concepts and Empirical Paradigms Based on Self-Organization, Embodiment and Coordination Dynamics* (World Scientific, Singapore).
37. Turvey MT (1990) *Am Psychol* 45:938–953.
38. Varela FJ, Lachaux J-P, Rodriguez E, Martinerie J (2001) *Nat Rev Neurosci* 2:229–239.
39. Perez Velazquez JL (2005) *Physica D* 212:161–182.
40. Başar E (2004) *Memory and Brain Dynamics: Oscillations Integrating Attention, Perception, Learning, and Memory*, Conceptual Advances in Brain Research (CRC Press, Boca Raton, FL), Vol 7.
41. Buzsaki G (2006) *Rhythms of the Brain* (Oxford Univ Press, Oxford).
42. Chen Y, Ding M, Kelso JAS (2003) *Exp Brain Res* 148:105–116.
43. Bressler SL, Kelso JAS (2001) *Trends Cognit Sci* 5:26–36.
44. Freeman WJ, Holmes MD (2005) *Neural Netw* 18:497–504.
45. Bressler SL, Tognoli E (2006) *Int J Psychophysiol* 60:139–148.
46. Friston KJ (1997) *NeuroImage* 5:164–171.
47. Kelso JAS (1991) in *Cardiorespiratory and Motor Coordination*, ed Koepchen HP (Springer-Verlag, Berlin), pp 224–234.
48. Kelso JAS, Bressler SL, Buchanan S, DeGuzman GC, Ding M, Fuchs A, Holroyd T (1992) *Phys Lett A* 169:134–144.
49. Mayville JM, Bressler SL, Fuchs A, Kelso JAS (1999) *Exp Brain Res* 127:371–381.
50. Wallenstein GV, Kelso JAS, Bressler SL (1995) *Physica D* 20:626–634.
51. Daffertshofer A, Peper CE, Beek PJ (2000) *Phys Lett A* 266:290–302.
52. Fuchs A, Deecke L, Kelso JAS (2000) *Phys Lett A* 266:303–308.
53. Fuchs A, Jirsa VK, Kelso JAS (2000) *NeuroImage* 11:359–369.
54. Haken H (1996) *Principles of Brain Functioning* (Springer, Berlin).
55. Oullier O, de Guzman GC, Jantzen KJ, Lagarde JF, Kelso JAS (2005) in *European Workshop on Movement Sciences: Mechanics-Physiology-Psychology*, eds Peham C, Schöllhorn WI, Verwey W (Sportverlag, Cologne, Germany), pp 34–35.
56. Richardson MJ, Marsh KL, Schmidt RC, (2005) *J Exp Psychol Hum Percept Perform* 31:62–79.
57. Beek PJ (1989) *Ecol Psychol* 1:55–96.
58. Carson RG, Riek S, Smethurst CJ, Lison-Parraga JF, Byblow WD (2000) *Exp Brain Res* 131:196–214.
59. Fink P, Foo P, Jirsa VK, Kelso JAS (2000) *Exp Brain Res* 134:9–20.
60. Kelso JAS (1984) *Am J Physiol* 246:R1000–R1004.
61. Kelso JAS, DelColle J, Schöner G (1990) in *Attention and Performance*, ed Jeannerod M (Erlbaum, Hillsdale, NJ), Vol XIII, pp 139–169.
62. Sternad D, Amazeen EL, Turvey MT (1996) *J Motor Behav* 28(3):255–269.
63. Swinnen SP (2002) *Nat Rev Neurosci* 3:348–359.
64. Turvey MT, Rosenblum LD, Schmidt RC, Kugler PN (1986) *J Exp Psychol Hum Percept Perform* 12:564–583.
65. Wimmers RH, Beek PJ, van Wieringen PCW (1992) *Hum Movement Sci* 11:217–226.
66. Mardia KV, Jupp PE (2000) *Directional Statistics* (Wiley, Chichester, UK).
67. Haken H, Kelso JAS, Bunz H (1985) *Biol Cybern* 51:347–356.
68. Williams JHG, Whiten A, Suddendorf T, Perrett DI (2001) *Neurosci Biobehav Rev* 25:287–295.
69. Wohlschläger A, Bekkering H (2002) *Exp Brain Res* 143:335–341.
70. Bonda E, Petrides M, Ostry D, Evans A (1996) *J Neurosci* 16:3737–3744.
71. Buccino G, Binkofski F, Fink GR, Fadiga L, Fogassi L, Gallese V, Seitz RJ, Zilles K, Rizzolatti G, Freund HJ (2001) *Eur J Neurosci* 13:400–404.
72. Grèzes J, Fonlupt P, Bertenthal B, Delon-Martin C, Segebarth C, Decety J (2001) *NeuroImage* 13:775–785.
73. Battelli L, Cavanagh P, Thornton IM (2003) *Neuropsychologia* 41:1808–1816.
74. Koski L, Iacoboni M, Dubeau MC, Woods RP, Mazziotta JC (2003) *J Neurophysiol* 89:460–471.
75. Saygin AP, Wilson SM, Hagler Jr DJ, Bates E, Sereno MI (2004) *J Neurosci* 24:6181–6188.
76. Hamilton AF, Grafton ST (2006) *J Neurosci* 26:1133–1137.
77. Grossman ED, Blake R (2001) *Vision Res* 41:1475–1482.
78. Grossman E, Batelli L, Pascual-Leone A (2005) *Vision Res* 45:2847–2853.
79. Wheaton KJ, Thompson JC, Syngeniotis A, Abbott DF, Puce A (2004) *NeuroImage* 22:277–288.
80. Pelphrey KA, Morris JP, Michelich CR, Allison T, McCarthy G (2005) *Cereb Cortex* 15:1866–1876.
81. Grossman ED, Donnelly M, Price R, Pickens D, Morgan V, Neighbor G, Blake R (2000) *J Cognit Neurosci* 12:711–720.
82. Steriade M, Llinas R (1988) *Physiol Rev* 68:649–742.
83. Mulholland T (1969) in *Attention in Neurophysiology*, eds Evans CR, Mulholland TB (Butterworth, London), pp 100–127.
84. Thut G, Nietzel A, Brandt SA, Pascual-Leone A (2006) *J Neurosci* 26:9494–9502.
85. Gastaut HJ (1952) *Rev Neurol (Paris)* 87:176–182.
86. Chatrian GE, Petersen MC, Lazarte JA (1959) *Electroencephalogr Clin Neurophysiol* 11:497–510.
87. Honaga E, Ukai S, Ishii R, Kawaguchi S, Yamamoto M, Ogawa A, Hirotsune H, Fujita N, Yoshimine T, Shinosaki K, *et al*. (2004) *Int Congress Ser* 1270:229–232.
88. Oberman LM, Hubbard EM, McCleery JP, Altschuler EL, Ramachandran VS, Pineda JA (2005) *Cognit Brain Res* 24:190–198.
89. Salenius S, Schnitzler A, Salmelin R, Jousmaki V, Hari R (1997) *NeuroImage* 5:221–228.
90. Nikouline VV, Linkenkaer-Hansen K, Wikstroem H, Kesaeniemi M, Antonova EV, Ilmoniemi RJ, Huttunen J (2000) *Neurosci Lett* 294:163–166.
91. Gaetz W, Cheyne D (2006) *NeuroImage* 30:899–908.
92. Pineda JA (2005) *Brain Res Rev* 50:57–68.
93. Blakemore SJ, Bristow D, Bird G, Frith C, Ward J (2005) *Brain* 128:1571–1583.
94. de Guzman GC, Tognoli E, Lagarde J, Jantzen KJ, Kelso JAS (2005) *Abstract Viewer/Itinerary Planner* (Soc Neurosci, Washington, DC).
95. Delgado MR, Frank RH, Phelps EA (2005) *Nat Neurosci* 8:1611–1618.
96. Jackson PL, Decety J (2004) *Curr Opin Neurobiol* 14:259–263.
97. Chatrian GE, Lettich E, Nelson PL (1985) *Am J EEG Technol* 25:83–92.
98. Picton W, Bentin S, Berg P, Donchin E, Hillyard S, Johnson R, Miller GA, Ritter W, Ruchkin DS, Rugg MD, *et al*. (2000) *Psychophysiology* 37:127–152.
99. Pfurtscheller G, Lopes da Silva FH, eds (1999) *Event-Related Desynchronization*, Handbook of Electroencephalography and Clinical Neurophysiology, Elsevier Science B.V.), Rev Ser, Vol 6.
100. Pritchard WS (1992) *Int J Neurosci* 66:119–129.
101. Gasser T, Sroka L, Mocks J (1986) *Psychophysiology* 23:704–712.
102. Hagemann D, Naumann E (2001) *Clin Neurophysiol* 112:215–231.
103. Van de Velde M, van Erp G, Cluitmans PJ (1998) *Electroencephalogr Clin Neurophysiol* 107:149–158.
104. Goncharova I, McFarland DJ, Vaughan TM, Wolpaw JR (2003) *Clin Neurophysiol* 114:1580–1593.
105. Wallstrom GL, Kass RE, Miller A, Cohn JF, Fox NA (2004) *Psychophysiology* 53:105–119.